ELSEVIER

Journal of Chromatography A, 690 (1995) 1–8

JOURNAL OF CHROMATOGRAPHY A

Axial dispersion in liquid magnetically stabilized fluidized beds

Motonobu Goto*, Takahiro Imamura, Tsutomu Hirose

Department of Applied Chemistry, Kumamoto University, Kumamoto 860, Japan

First received 9 August 1994; revised manuscript received 17 October 1994; accepted 17 October 1994

Abstract

Magnetic stabilization permits the expansion of a packed bed without mixing of solid particles. This allows operation with a low pressure drop, free from clogging, and high column efficiency. The performance of magnetically stabilized fluidized beds (MSFB), developed for affinity separation, was studied in terms of axial dispersion, the controlling factor in column efficiency. Porous beads of chitosan-containing magnetite particles were used as the stationary phase. Bed expansion increased with increase in flow-rate and with decrease in magnetic field strength. The axial dispersion coefficient was evaluated by moment analysis of the impulse response curves. The axial dispersion for the MSFB was comparable to that of a packed bed and smaller than that of a fluidized bed. The chromatographic behaviour of the MSFB was consistent with the above results.

1. Introduction

The use of a magnetically stabilized fluidized bed (MSFB) is an alternative to conventional column operation, such as with a packed bed (PB) or fluidized bed (FB), for the large-scale purification of biological products. The fluidization is stabilized by a magnetic field so that the bed can be maintained in a quiescently fluidized state without turbulent solids mixing. The MSFB has advantages of both packed and fluidized beds, such as efficient fluid–solid contact, low pressure drop, resistance to clogging and continuous counter-current operation.

The performance of the MSFB has been studied for both gas [1] and liquid [2] systems. The MSFB behaves like a packed bed but has lower operational pressure drops while still having sharp breakthrough and narrow elution bands of solute with high column capacity [1]. The application of a magnetic field to a liquid fluidized bed produces several different operating regimes depending on the liquid velocity and the strength of the magnetic field. There exists an operating regime termed "stabilized" where the bed is fluidized without mixing motion of the particles. The adsorption efficiency for the bed may be defined by the dynamic capacity adsorbed until the breakthrough point, which depends on the shape of the breakthrough curve. In that regime, the adsorption efficiency would be higher than for a conventional fluidized bed, because of the smaller axial dispersion without mixing of particles in the bed.

The adsorption efficiency decreased due to the band spreading resulting from axial dispersion and rate processes, such as intraparticle diffusion, external fluid–solid mass transfer and in-

* Corresponding author.

0021-9673/95/$09.50
SSDI 0021-9673(94)00993-7

trinsic adsorption rate. The intraparticle diffusion and intrinsic adsorption rate are inherent in the adsorbate–adsorbent system. As external mass transfer is not usually dominant, the evaluation of the axial dispersion is most important for the analysis of adsorption systems.

The objective of this paper is to evaluate axial dispersion in the MSFB in comparison with the PB and the FB. The axial dispersion reported in the literature was measured for nickel powder on a relatively small scale (solid 95 or 20–45 μm, column 6.35 and 9.53 mm I.D.) [3] and for steel spheres on a relatively large scale (spheres 30–140 mesh, column 76.2 mm I.D.) [2] as a solid. We have measured the axial dispersion coefficient with porous adsorbent particles that had been prepared for affinity separation of trypsin or lysozyme [4].

2. Experimental

2.1. Preparation of magnetic adsorbent

A magnetic affinity adsorbent was prepared from chitosan. As chitosan is a very hydrophilic polysaccharide and has amino groups, it is suitable as an affinity adsorbent.

Magnetite fine particles were synthesized from iron(II) sulfate by moderate oxidation with potassium nitrate in the presence of ammonia under a nitrogen atmosphere at boiling temperature. The average diameter of the magnetite particles obtained was 580 nm.

Magnetite-containing porous chitosan beads were prepared as follows. Chitosan (from crab shells; Sigma) was dissolved in 4% acetic acid to obtain a 3% (w/v) chitosan solution. After filtration and degassing, the chitosan solution was mixed with the magnetite particles prepared as above. The mixture was forced into a nitrogen stream through a needle nozzle by means of the aerosol jet technique [5]. The sol particles extruded from the nozzle were immediately gelled in sodium hydroxide solution located about 0.10 m downstream from the jet nozzle. After the magnetic chitosan beads had been sufficiently washed with water, the beads were cross-linked with glutaraldehyde. The size of the beads could be controlled by the chitosan concentration, extrusion speed, nozzle size and nitrogen flow-rate. The average diameter of the particles used was 0.550 mm with a standard deviation of 0.0787 mm. The content of the magnetite was 5% (w/v). The apparent density of the adsorbent was 1210 kg/m^3 and the void fraction was 0.911. The minimum fluidizing velocity was $0.90 \cdot 10^{-3}$ m/s.

The prepared adsorbent was used for the affinity adsorption of lysozyme by a group-specific affinity interaction with the glucosamines of the chitosan matrix, and of trypsin after introducing soy bean trypsin inhibitor as a ligand [4].

2.2. Impulse response measurement

The experimental apparatus is shown schematically in Fig. 1. The column was a C10/20 (200 mm × 10 mm I.D.) (Pharmacia–LKB Biotechnology) with an adapter that allowed adjustment of the bed height. The position of the adapter was controlled at the top of the fluidized bed so as to eliminate the dead space above the bed. For packed-bed operation, the adapter was controlled at the top of the unfluidized bed so as to prevent expansion of the bed. The column was cooled at 277 K with a water-jacket. A magnetic field was applied collinear with that of the mobile phase by surrounding the column with two wire-wound solenoid electromagnets. D.c. power was supplied by a regulated d.c.

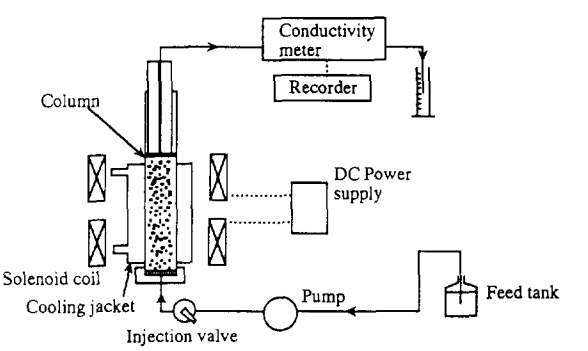

Fig. 1. Experimental apparatus for magnetically stabilized fluidized bed operation.

power supply (Model GP035-10; Takasago, Tokyo, Japan) and the magnetic field strength was controlled by the current applied. The solenoid coil (30 mm × 68 mm I.D.) consisted of approximately 550 turns of 1-mm copper wire. The fluidizing liquid flow was provided by an HPLC pump (Model PU-880; JASCO, Tokyo, Japan).

All the experiments were carried out in the "flow-first" mode [2] where the bed was fluidized by first flowing the liquid and then applying a magnetic field. The "flow-first" mode was better than the "field-first" mode with regard to reproducibility. A 25-μl pulse of aqueous 40 m*M* NaCl solution was injected into the column with a seven-port injection valve (Pharmacia–LKB Biotechnology). The response of the pulse was measured with an electric conductivity meter (Model 213A; Wescan Instruments, Santa Clara, CA, USA). The response curve recorded was analysed by the moment method. The magnetic field applied was 25 kA/m unless stated otherwise. NaCl was chosen as a tracer because the adsorption of Na^+ and Cl^- ions is weak or negligible even if they diffuse into the particles.

2.3. Affinity chromatography

Purification of lysozyme was demonstrated by the magnetically stabilized fluidized bed filled with the magnetic chitosan beads. Lysozyme dissolved in 0.1 *M* Tris–HCl buffer solution (pH 7.4) was used as a feed solution. The feed solution was supplied to the column until the adsorbent was saturated with lysozyme. Then, the lysozyme adsorbed was eluted with a 0.1 *M* acetic acid. The magnetic field applied was 25 kA/m.

3. Results and discussion

3.1. Behaviour of magnetically stabilized fluidized bed

Without a magnetic field, the particles in the bed became fluidized at the minimum fluidizing velocity, and moved within the bed as it expanded. With a magnetic field, the bed started to expand at the minimum fluidizing velocity but without relative motion of the particles (stably fluidized). When the flow-rate was increased further, the bed height increased and the particles started to move (unstably fluidized).

The behaviour of the magnetic fluidized bed was classified from visual observation of different regimes depending on the strength of the magnetic field and the flow-rate as shown in Fig. 2. The bed changed from an unfluidized bed (dense packed) to a stably fluidized bed (quiescent) and then finally an unstably fluidized bed (turbulent solids mixing) regime as the flow-rate increased at a given magnetic field. The particles in the stable regime were fixed in place in the expanded bed where the void volume is larger than that in the packed bed, that is, the particle motion is arrested. On the other hand, particles move in a circulatory manner in the bed with turbulent liquid flow in the unstably fluidized regime. The particle behaviour in the unstably fluidized state was "gulf streaming" [3] or "circulatory motion of the overall bed" rather than "roll cell" motion [2]. The behaviour shifted from gulf streaming to circulatory motion and finally to random motion as the flow-rate increased.

Ideal performance of the fluidized-bed operation may be attained by minimizing bed expansion and extending the stably fluidized state to

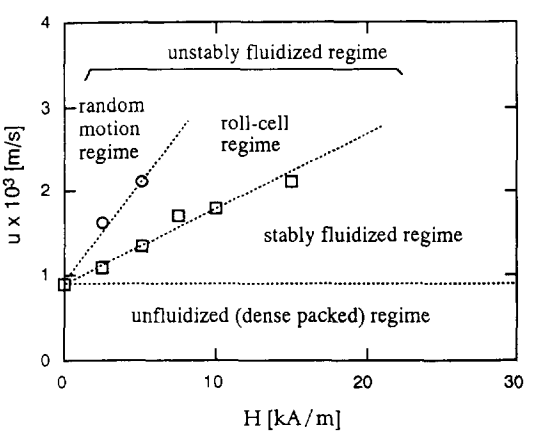

Fig. 2. Effect of magnetic field strength on the fluidization characteristics of bed (packed-bed length = 0.0647 m). ○ = Transition between random motion and roll-cell regime; □ = transition between roll-cell and stably fluidized regime.

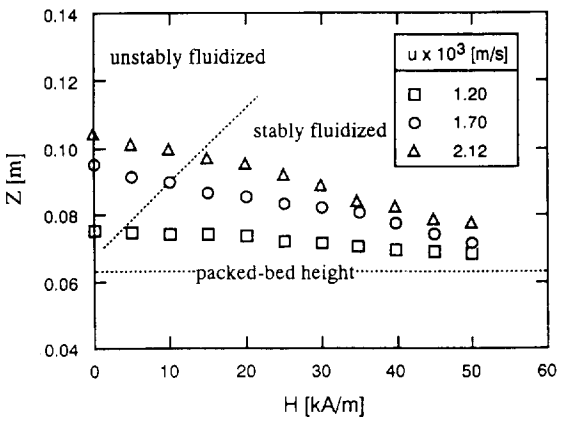

Fig. 3. Effect of magnetic field strength and flow-rate on the fluidized bed length.

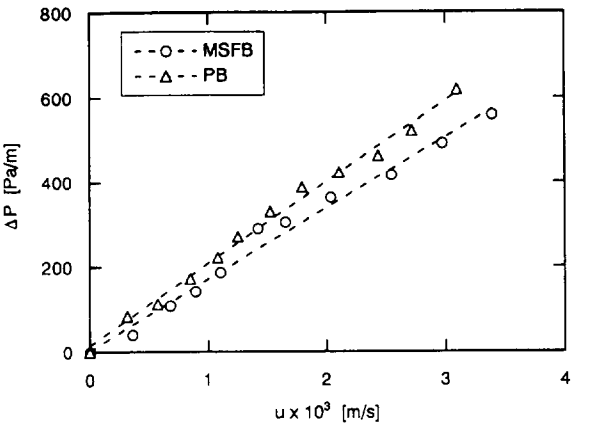

Fig. 4. Comparison of pressure drops between the MSFB and PB.

higher flow-rates while maintaining a low pressure drop. Fig. 3 shows the expansion of the bed as a function of the magnetic field strength and the flow-rate. Larger bed heights were observed for higher flow-rates. The bed expansion decreased as the magnetic field increased. The largest decrease in the bed height was observed in the unstable regime. Once the bed had stabilized, its height did not decrease further with increasing magnetic field. The magnetic field extended the quiescent state to higher flow-rates, decreased bed expansion and minimized axial mixing by inhibiting axial motion of the particles. This behaviour may result in higher efficiency of adsorption in the bed.

3.2. Pressure drops

Pressure drops in the PB and MSFB are shown in Fig. 4. The pressure drop in the MSFB was smaller than that in the PB because of the larger bed voidage. As the column size was relatively small and the particle size was large, the pressure drop was not large in this experiment. As the pressure drop is a function of bed voidage, particle size and flow-rate [6], a larger bed voidage leads to a smaller pressure drop. If the particle size were much smaller, the pressure drop in the PB would be much larger.

In addition to the lower pressure drop, the MSFB can avoid consolidation of the bed. One of the problems with chromatography using a soft gel as the stationary phase is consolidation of the bed at higher flow-rates, resulting in a significant increase in pressure drop [7]. As particles in the MSFB are fixed in the bed with a large bed voidage by a magnetic field even at high flow-rates, consolidation of the bed does not occur. Therefore, a soft gel can be used without consolidation at high flow-rates.

3.3. Impulse response analysis

The theoretical model developed for a packed bed is not strictly applicable to a fluidized bed system, because the adsorbent particles move in the bed so that there is axial mixing of solids in addition to fluid mixing. However, a packed-bed model was used in order to compare the behaviours among the PB, FB and MSFB.

The impulse response in a packed column is governed by a system of coupled partial differential equations which include axial dispersion, external fluid–particle mass transfer and intraparticle diffusion [8]. On the assumption of linear adsorption equilibrium, the moments can be derived [9]. The first absolute and the second central moments of the response curve for the system are

$$\mu_1' = \frac{z}{v}\left[1 + \frac{1-\varepsilon_B}{\varepsilon_B}\cdot K\right] + \frac{t_0}{2} \qquad (1)$$

$$\mu_2 = \frac{2z}{v}\left[\frac{1-\varepsilon_B}{\varepsilon_B}\cdot\frac{K^2R^2}{3}\left(\frac{1}{5D_e}+\frac{1}{k_fR}\right) + \frac{D_{ax}}{v^2}\left(1+\frac{1-\varepsilon_B}{\varepsilon_B}\cdot K\right)^2\right] + \frac{t_0^2}{12} \quad (2)$$

The first absolute moment, μ_1', characterizes the position of the centre of gravity of the response peak, whereas the second central moment, μ_2, characterizes the width of the peak.

The first and second moments of the experimental response curve are calculated by

$$\mu_1' = \int_0^\infty Ct\,dt \Big/ \int_0^\infty C\,dt \quad (3)$$

$$\mu_2 = \int_0^\infty C(t-\mu_1')^2\,dt \Big/ \int_0^\infty C\,dt \quad (4)$$

The governing equations were solved analytically [10] in the time domain and the analytical solution was given in terms of an infinite integral.

The response curves are compared in Fig. 5 among the PB, FB and the MSFB at a flow-rate of $3.6\cdot10^{-4}$ m/s. The peaks for the MSFB and FB eluted later than that for the PB because of larger bed void space. The shapes of the curves were similar between the PB and the MSFB. The peak for the FB was broader than the other two peaks. Hence, the axial dispersion for the MSFB and PB were almost the same and that for the FB was larger.

The height equivalent to a theoretical plate (HETP), H, reduced HETP, h, and plate number, N, are given by

$$H = z\mu_2/\mu_1'^2 \quad (5)$$

$$N = \mu_1'^2/\mu_2 \quad (6)$$

$$h = H/2R \quad (7)$$

The HETP and the reduced HETP are shown in Fig. 6. The FB had the largest HETP owing to the large axial dispersion. The HETPs for the MSFB and PB were comparable. As the bed was expanded for the MSFB, the HETP was even smaller than that for the PB. The reduced HETP seems to be larger than typical value ($h = 2$–3), because the operation was not optimum.

3.4. Parameter evaluation for packed bed

To evaluate the axial dispersion coefficient, D_{ax}, unknown parameters, K, D_e and k_f, in the second moment must be previously determined. Values of the bed length, z, and the bed porisity, ε_B, are constant for the PB, whereas they are a function of flow-rate for the FB and the MSFB. Thus, the linear regression analysis where the moments are plotted against inverse of the flow-rate to give a straight line is not applicable for the FB and MSFB. Therefore, the parameters K and D_e were first obtained from the experiment

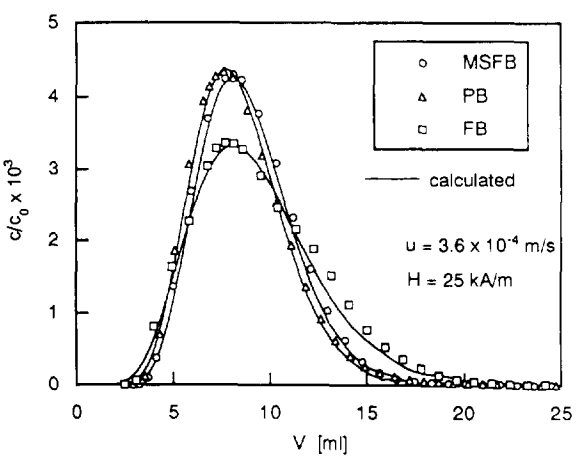

Fig. 5. Comparison of impulse response curve among the MSFB, PB and FB.

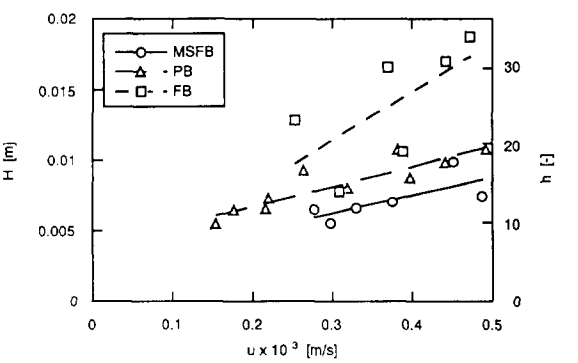

Fig. 6. Comparison of HETP and reduced HETP among the MSFB, PB and FB.

for the PB, because these parameters should be inherent in the adsorbent regardless of the bed state.

The adsorption equilibrium constant, K, was first calculated from the first moment, μ_1'. The slope of the regression line in the plot of $(\mu_1'-t_0/2)$ versus z/v was $1+(1-\varepsilon_B)K/\varepsilon_B$, which gave $K=1.15$. This value includes the effect of pore volume and intrinsic adsorption at the inner surface.

When the influence of external mass transfer on the second moment is small, the second moment can be analysed by the linear regression method from the plot of $(\mu_2-t_0^2/12)v/(2z)$ versus $1/v$. As the contribution of k_f is not expected to be negligible and then the mass transfer term in second moment is a function of the flow-rate, the parameters, D_e and D_{ax} were estimated by non-linear regression. The external mass transfer coefficient, k_f, was estimated by a correlation proposed by Wakao and Kaguei [11] where diffusivity of NaCl was estimated by the Nernst–Haskell equation [12].

The axial dispersion coefficient is usually proportional to the flow-rate for liquid systems except for extremely small flow-rates where molecular diffusion has an influence. Hence, the value of D_{ax}/v was assumed to be constant. D_e and D_{ax}/v were evaluated to be $8.59\cdot10^{-10}$ m^2/s and $1.51\cdot10^{-3}$ m, respectively for the PB.

3.5. Axial dispersion coefficient for a fluidized bed and a magnetically stabilized fluidized bed

For the evaluation of the axial dispersion coefficient of the FB and MSFB, the values of K and D_e determined from the PB were used. The axial dispersion coefficient was calculated from the second moment, Eq. 2, by direct substitution of z, ε_B, K, D_e and k_f for each run at various flow-rates. The bed voidage was calculated from the bed height for the packed state and the fluidized state; the bed voidage for the PB was 0.429.

The axial dispersion coefficients obtained are shown as a function of flow-rate in Fig. 7. As the axial dispersion coefficient for the PB was estimated by linear regression of the entire data, the result for the PB is represented as a straight line. It is evident that the axial dispersion for the MSFB is nearly the same as for the PB, whereas the axial dispersion coefficient for the FB is larger than that for the PB and MSFB. The FB has a large axial dispersion coefficient, because of the mixing of fluid induced by the movement of solid particles. As the solid particles are fixed by the magnetic field for the MSFB, the mixing of fluid for the MSFB is similar to that for the PB. The only difference between the PB and MSFB is the bed voidage. A larger bed voidage results in a lower pressure drop and avoidance of clogging problems of the bed caused by suspended solids in the feed solution.

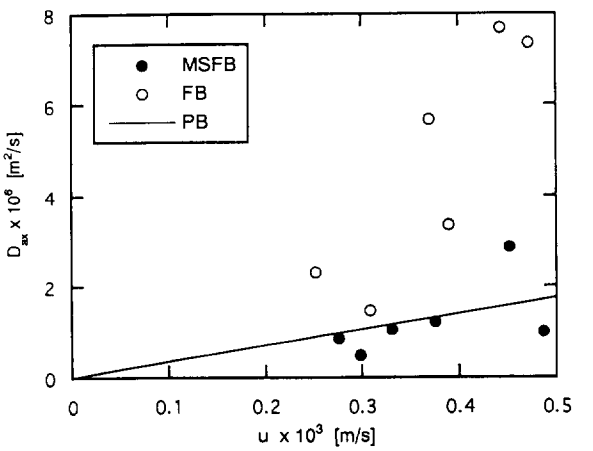

Fig. 7. Comparison of axial dispersion coefficient among the MSFB, FB and PB.

The axial dispersion coefficient is shown in dimensionless form as Pe^{-1} versus Re in Fig. 8. Literature data [2,3,13] are given for comparison. The region of Reynolds number in this work is located in the same region as reported by Goetz and Graves [3]. One of the main differences between this work and the literature [1,12] is that porous chitosan particles were used here whereas non-porous metal particles were used by others [2,3]. The Peclet number obtained in this work almost coincides with the published values. The axial dispersion for the MSFB is nearly the same as for the PB, as reported previously [2,3].

The response curves were simulated with the parameters obtained by moment analysis. An

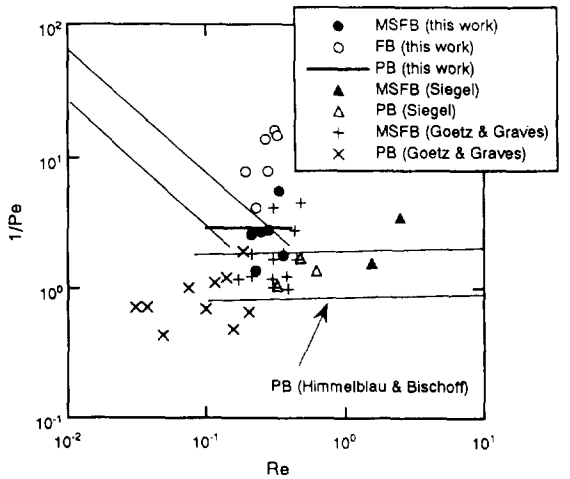

Fig. 8. Comparison of $1/Pe$ with literature data (Siegell [2]; Goetz and Graves [3]; Himmelblau and Bischoff [13]).

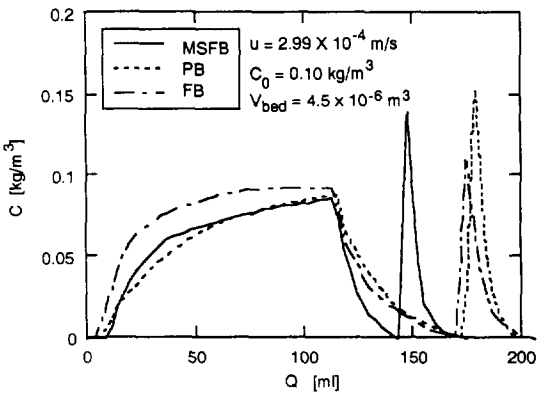

Fig. 9. Comparison between the MSFB, PB and FB with respect to the performance of affinity separation of lysozyme by magnetic chitosan beads.

analytical solution [10] was used for the simulation. The solid lines in Fig. 5 indicate the calculated curves. The agreement between the experimental and calculated curves indicates that the parameters obtained by moment analysis were reliable.

3.6. *Affinity chromatography*

An affinity separation, which consisted of a series of adsorption, washing and elution steps, was carried out, for lysozyme with the magnetic chitosan beads. The histories of the effluent lysozyme concentration during the operation are compared among the MSFB, FB and PB in Fig. 9. As the adsorbent beads were fixed in the bed by magnetic force, the performance of the MSFB was almost the same as for the PB and better than for the FB. The breakthrough curve in the adsorption step was slightly gentler for the MSFB than that for the PB because of the larger bed voidage. The amounts of adsorbed lyozyme were $0.306 \cdot 10^{-3}$, $0.278 \cdot 10^{-3}$ and $0.181 \cdot 10^{-3}$ g/cm^3 bed for the PB, MSFB and FB, respectively, under the same conditions. Hence, the efficiency of the adsorption for the MSFB is located between those for the PB and FB. The result agrees with the axial dispersion behaviour. As the particle size used in this study is relatively large, the mass transfer resistance in a particle may dominate. For smaller particles, the difference between the MSFB and FB must be large, because axial dispersion may have a considerable influence on peak broadening.

4. Conclusion

The performance of the MSFB was evaluated in terms of the axial dispersion in the bed. The impulse response measured was analysed by the moment method. The axial dispersion coefficient obtained for the MSFB was comparable to that for the PB and smaller than that for the FB. Therefore, the performance of the MSFB was similar to that of the PB.

As the MSFB is aimed at large-scale preparative operation, the system used in this work may not be suitable for practical operation where larger columns and smaller particles may be used. The advantages of the MSFB may become evident for practical systems. Further work is needed for systems close to a practical scale.

Symbols

C Concentration (M)
D_{ax} Axial dispersion coefficient (m^2/s)
D_e Intraparticle effective diffusivity (m^2/s)

H Magnetic field strength (kA/m)
K Adsorption equilibrium constant
k_f Fluid-to-particle mass transfer coefficient (m/s)
Pe $=2R\,v/D_{ax}$; Peclet number
R Particle radius (m)
Re $=2R\,v\rho/\mu$; Reynolds number
t Time (s)
t_0 Injection time (s)
u Superficial fluid velocity (m/s)
V Effluent volume (m^3)
v Interstitial fluid velocity (m/s)
z Bed height (m)
ε_B Bed void fraction
μ Fluid viscosity (kg/m s)
μ_1' First absolute moment (s)
μ_2 Second central moment (s^2)
ρ Fluid density (kg/m^3)

Acknowledgements

Financial support from the Miyajima Toshiharu Foundation is gratefully acknowledged. The authors are grateful to Mr. S. Morisaki for experimental assistance.

References

[1] R.E. Rosensweig, *Science*, 204 (1979) 57.
[2] J.H. Siegell, *Powder Technol.*, 52 (1987) 139.
[3] V. Goetz and D.J. Graves, *Powder Technol.*, 64 (1991) 81.
[4] M. Goto, T. Imamura and T. Hirose, in M. Suzuki (Editor), *Fundamentals of Adsorption –Proceedings of the IVth International Conference on Fundamentals of Adsorption*, Kodansha, Tokyo, 1993, p. 227.
[5] C.H. Lochmüller and L.S. Wigman, *Sep. Sci. Technol.*, 22 (1987) 2111.
[6] R.M. Nicoud and M. Perrut, *Chromatographic and Membrane Processes in Biotechnology*, Kluwer, Dordrecht, 1991, p. 53.
[7] E. Sada, S. Katoh and M. Shiozawa, *Biotechnol. Bioeng.*, 24 (1982) 2279.
[8] M. Goto, N. Hayashi and S. Goto, *Sep. Sci. Technol.*, 18 (1983) 475.
[9] M. Kubin, *Collect. Czech. Chem. Commun.*, 30 (1965) 1104, 2900.
[10] A. Rasmuson and I. Neretnieks, *AIChE J.*, 26 (1980) 686.
[11] N. Wakao and S. Kaguei, *Heat and Mass Transfer in Packed Beds*, Gordon and Breach, New York, 1982.
[12] R.C. Reid, J.M. Prausnitz and B.E. Poling, *The Properties of Gases and Liquids*, McGraw-Hill, New York, 4th ed., 1987.
[13] D.M. Himmelblau and K.B. Bischoff, *Process Analysis and Simulation*, Wiley, New York, 1967.